Available online at www.sciencedirect.com

SciVerse ScienceDirect

Ceramics International 39 (2013) 6333–6342

CERAMICS INTERNATIONAL

www.elsevier.com/locate/ceramint

Effect of dual reinforced ceramic particles on high temperature tribological properties of aluminum composites

Suresh Kumar, Ranvir Singh Panwar, O.P. Pandey*

School of Physics and Materials Science, Thapar University, Patiala-147004, Punjab, India

Received 7 November 2012; received in revised form 18 January 2013; accepted 19 January 2013
Available online 1 February 2013

Abstract

The nature and distribution of hard ceramic particles in composite materials influences the properties to greater extent. In the present work, the role of hard ceramic reinforced particles on the tribological behaviour of aluminum metal matrix composites consisting of single (SRP) and dual reinforced particles (DRP) is studied at different temperatures. Zircon sand and silicon carbide particles of size 20–32 μm were used as reinforcement in commercial grade LM13 piston alloy. Composites of dual reinforced particles in aluminum matrix (DRP-AMCs) were developed by mixing 15 wt% reinforced particles by two step stir casting technique. The wear behaviour of DRP-AMCs and SRP-AMCs (single reinforced particles aluminum matrix composite) was investigated using a pin-on-disc method at high temperatures under dry sliding condition. The microstructural examination of developed composites shows globular and finely distributed eutectic silicon in the vicinity of the reinforced particles. Metallographic investigation revealed that the wear zone of the SRP composite consisted of a hardened layer, which is responsible for high wear loss observed in the SRP composite. The results further indicate a transition in the wear mode that occurs after 150 °C for all composites. Study reveals that the dual reinforcement of particles enhances the wear resistance as compared to single reinforced particles if mixed in a definite ratio. A combination of 3% zircon sand and 12% silicon carbide particle reinforced composite exhibits better wear resistance as compared to other combinations at all the temperatures for low and high loads both.

Keywords: Aluminum matrix composite; Wear; Debris; SEM

1. Introduction

Aluminum matrix composites (AMCs), particularly hybrid AMCs are finding increased applications in various sectors of transportation industries such as brake drums, engine pistons and other components because of the high strength, low density, corrosion resistance, wear resistance and easy workability.

In recent years, few attempts have been made to develop hybrid AMCs reinforced with SiC, Al_2O_3 and graphite or in combination of the above [1–3]. The room temperature sliding wear behavior of Al_2O_3 and SiCp reinforced aluminum matrix hybrid composites under both, the dry and lubricant conditions have been investigated by Wang et al. [4] and reported the improvement in tribological properties of hybrid composites. The dry sliding wear behavior of Al based composites reinforced with Gr and SiC particulate up to 10 wt% was studied at room temperature by Suresha et al. [5]. They have reported that Al–SiC–Gr hybrid composite exhibits better wear resistance. The role of magnesium addition along with SiC and Al_2O_3 particles on dry sliding wear behavior of the aluminium matrix hybrid composites at room temperature indicate that wear resistance of the composites increased with increasing Mg addition [6].

Das et al. [7] have compared the wear properties of alumina and zircon sand reinforced AMCs and reported that decrease in particle size improves wear resistance at room temperature. Ahmad et al. [8] studied the effect of particle size for Al_2O_3 reinforced AMCs and reported that the fine particle reinforced composites have higher hardness as compared to coarse particles. This is because composites reinforced with the finer particle size offer

*Corresponding author. Tel.: +91 1752393130; fax: +91 1752393005.
E-mail address: oppandey@thapar.edu (O.P. Pandey).

0272-8842/$ - see front matter © 2013 Elsevier Ltd and Techna Group S.r.l. All rights reserved.
http://dx.doi.org/10.1016/j.ceramint.2013.01.059

higher number of barriers per unit volume compared with composites reinforced with larger particle size at the same weight percentage. Ozdemir and Yakuphanoglu [9] have reported that the fine particle reinforced composites also exhibit better thermal conductivity as compared to coarse particles reinforced composite. In all the above work, the hybrid composites have been developed by single step stir casting routes. As compared to single step stir casting route the two-step stir casting method has an advantage in terms of promoting wettability, reduction of porosity and homogeneous distribution of reinforced particles, which provide better tribological properties [10,11]. In earlier reported two-step stir casting method the mixing of particles is done in semisolid state by manually stirring with steel rod, which is cumbersome process and also the agglomeration of fine particles occurs [12].

Considering all these parameters, this study is aimed to analyze the combined effect of both fine size zircon sand and silicon carbide particle reinforcement in commercial grade aluminum alloy composite. In the present work two step stir casting route is adopted for the development of hybrid composite. For the reinforcement a combination of zircon sand and silicon carbide particles in a defined ratio has been taken to develop composite as this combination is not studied so far. The wear behavior of the developed composites has been studied at different temperatures with variation in load.

2. Experimental details

2.1. Charged materials

Zircon sand ($ZrSiO_4$) and silicon carbide (SiC) were used as reinforcement in LM13 piston alloy. LM13 alloy was obtained in the form of ingots. The compositional analysis of the LM13 alloy was done by wet chemical analysis, which is given in Table 1.

2.2. Melting and casting

The required quantity of LM13 alloy was melted in a graphite crucible at 750 °C in an electric resistance furnace. The melt was stirred at a speed 630 rpm using a graphite impeller to create vortex inside the melt. Zircon sand and silicon carbide particles of fine size (20–32 μm) were selected for present work. The ceramic particles for reinforcement were taken in defined proportion and mixed properly before charging. Particles prior to mixing were preheated at 450 °C to drive off the moisture. After the formation of vortex in the melt, the particles were charged near vortex with the help of funnel kept on top of vortex at the rate of 20–25 g min^{-1} into the melt. After mixing of particles, the melt slurry is allowed to solidify in a graphite crucible at room temperature. The solidified mass was again re-melted in the furnace. This molten mass was again stirred for 12–15 min. During fabrication of composites, the amount of LM13 alloy, stirring duration and position of stirrer in the crucible were kept constant to minimize the contribution of variables related to stirring on distribution of second phase particles. The details of experimental condition are given in Table 2.

Table 1
Chemical composition of LM13 alloy.

Elements	Si	Fe	Cu	Mn	Mg	Zn	Ti	Ni	Pb	Sn	Al
wt%	11.8	0.3	1.2	0.4	0.9	0.2	0.02	0.9	0.02	0.005	Balance

Table 2
List of processing parameters.

Parameter	1st step	2nd step
Melting temperature	750 °C	800 °C
Total stirring time	22–25 min	5 min
Mixing time	8–10 min	5 min
Blade angle	45°	45°
No. of blades	3	3
Position of stirrer in the melt	Up to 2/3 depth	Up to 2/3 depth

Table 3
Reinforced combination of composites.

Composite	Total 15 wt% reinforcement	
	$ZrSiO_4$	SiC
A	15	–
B	3.75	11.25
C	7.5	7.5
D	11.25	3.75
E	–	15

In our earlier work it was observed that 15 wt% reinforcement has given better property, so we have restricted the reinforcement up to 15 wt% only [13–15]. Moreover, this is also in accordance with as reported work by Okafor and Aigbodion [16]. In order to compare and correlate the effect of dual reinforcement of particles on mechanical and tribological properties, five different composites containing a total of 15 wt% reinforcement in different proportion of zircon sand and silicon carbide were fabricated and have been designated by alphabets as given in Table 3.

Dry sliding wear tests of the reinforced and unreinforced alloys were performed in between 50 °C and 300 °C at an interval of 50 °C using a pin-on-disc wear and friction monitor (Model TR-20, Ducom, Bangalore). The relative humidity during the test was observed to vary between 25% and 35%. The cylindrical shaped samples (30 × 8 mm) of composite were tested against the hardened EN32 steel disc having hardness 65 HRC. Before testing, each specimen was ultrasonically cleaned in acetone. The wear test of specimen from each set of composite was done up to 2880 m of sliding distance at a constant sliding velocity of 1.6 m s^{-1} and at different loads. Wear rate for the pin is calculated from the volume loss of materials. The microstructural analysis has been done with the help of both optical (Eclipse MA-100, Nikon) and scanning

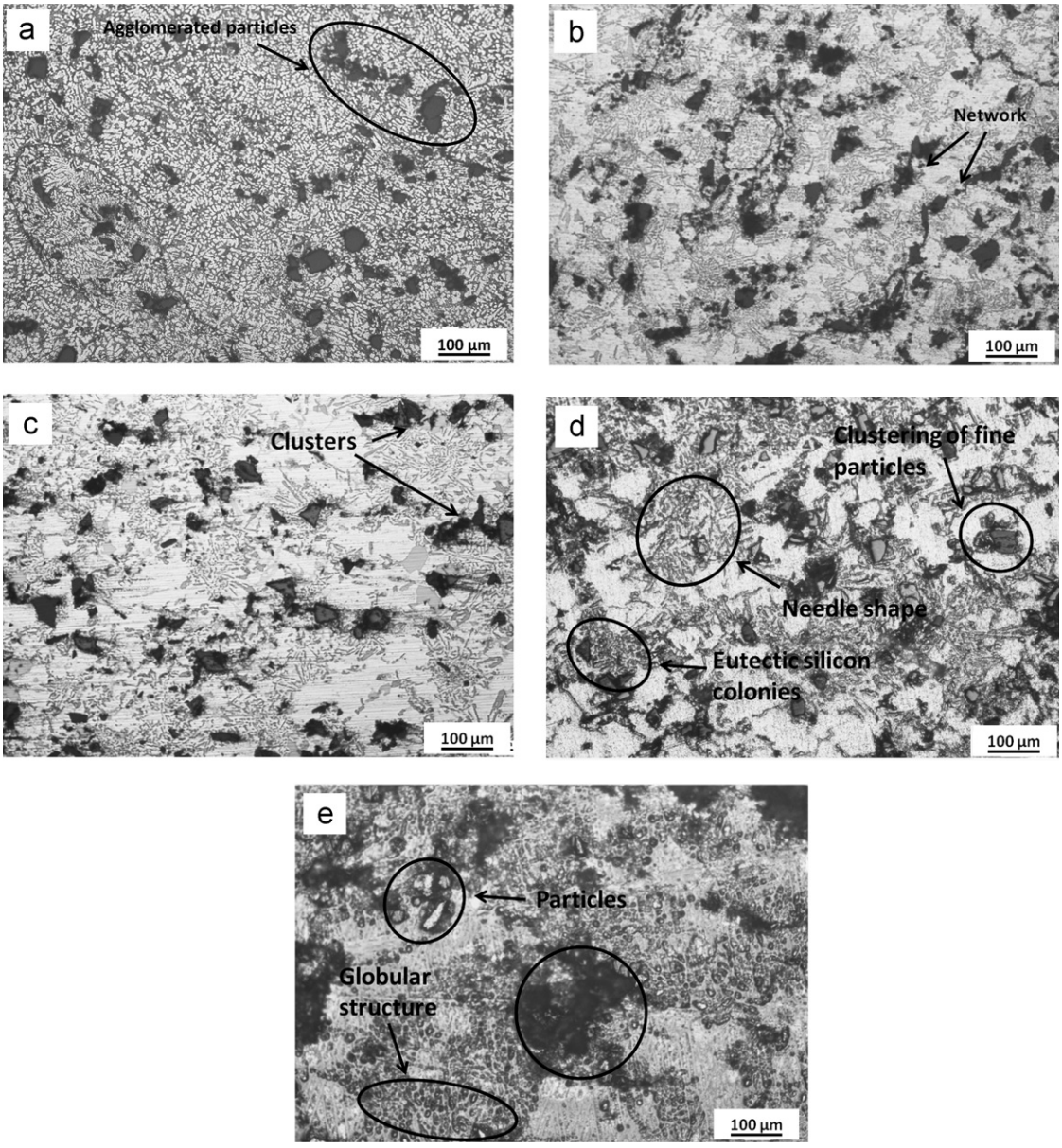

Fig. 1. The optical micrograph of composites at 200X (a) Composite-A, (b) Composite-B, (c) Composite-C, (d) Composite-D and (e) Composite-E.

electron microscope (JEOL, JSM-6510LV, Japan) at various magnifications. Before optical observation the sample was mechanically polished and etched by Keller's reagent for obtaining better contrast. Microhardness at different phases was measured by Vickers hardness testing machine (Mitutoyo, Japan). Microhardness measurement was done on each set of sample by taking minimum of ten indentations per sample at 100 gf load.

3. Results and discussion

3.1. Microstructural analysis

Optical microscopy was used to investigate the microstructural modifications induced by the two-step stir casting process in the $ZrSiO_4$ and SiC reinforcement composites. The optical micrograph of the composites is shown in Fig. 1(a)–(e). Dendritic structure got modified during casting, which is influenced by many factors such as dendritic fragmentation, restriction of dendritic growth by the particles and thermal conductivity mismatch between the particles and melt. Ceramic particles also act as a barrier for the dendritic growth and this phenomenon is more pronounced if the cooling rate is high. Panwar and Pandey [17] in their work reported that the particles can be assumed to act as a barrier to the dendritic growth.

The optical micrographs of composite-A reinforced with 15 wt% zircon sand particles are shown in Fig. 1(a). This figure shows homogeneous distribution of particles in AMCs, which is desired for achieving better wear and mechanical properties. Due to the high shear rate during stirring, particles get distributed throughout the melt, which also minimizes the

particles settling. However, fine particles are pushed at faster rate during stirring action which gets agglomerated around the area away from stirrer which is visible at certain places in the microstructure. In the micrograph of the composite-A fragmented dendrites in the matrix can also be seen, though limited dendritic growth in the particle depleted region is also visible in this figure. During solidification fine size (20–32 μm) zircon sand particles are pushed or engulfed by advancing solid–liquid interface creating sufficient space inside the matrix, which leads to growth of dendrite [11]. Dendrites fragmentation can be attributed to the shearing of initial dendritic arms by the stirring action. The zircon sand particles provide site for nucleation of melt as temperature difference between particle and the melt is higher. It was also found that the perturbation in the solute field due to the presence of particles can change the dendrite tip radius and the dendrite tip temperature. All these effects lead dendrite to cell formation. Also the length of the dendrite is reduced due to the presence of the particles in matrix [18]. The optical micrographs of composite-B reinforced with 3.75 wt% of zircon sand and 11.25 wt% silicon carbide particles in the ratio of 1:3 are shown in Fig. 1(b). The structure exhibits uniform distribution of particles inside the matrix. However, the particles are observed to form network structure at certain places. Moreover, eutectic silicon network is fine and the dimension of interdendritic region is comparably less than that of the particle diameter. Absence of voids at interface indicates the good bonding between the matrix and the reinforced particles, which helps in better load transfer from the matrix to reinforcement materials.

The optical micrographs of composite-C containing 7.5 wt% of zircon sand and 7.5 wt% silicon carbide particles in the ratio of 1:1 is shown in Fig. 1(c). It depicts the refinement of microstructure and eutectic silicon. The eutectic silicon got refined to finer scale and nucleates near particles as colonies. Clustering of particles is observed at some places and some of the clustered particles have chip out during grinding and polishing of the samples.

Micrograph of composite-D containing 11.25 wt% of zircon sand and 3.75 wt% silicon carbide particles in the ratio 3:1 is shown in Fig. 1(d). Finer to coarse distribution of eutectic silicon along with homogeneous distribution of particles can be seen. Eutectic silicon colonies around particles are more pronounced in the micrograph. Eutectic silicon is more refined and morphology has changed from acicular to globular around the particles. Also in the matrix the eutectic silicon having blunted morphology as compared to long needle shape or acicular is seen. However, the fine particles and silicon form a network structure because of pushing interface from different nucleation sites. Moreover, the clustering of fine particles at some places is also observed.

Optical micrograph of composite-E containing 15 wt% of silicon carbide particles is shown in Fig. 1(e). Here eutectic silicon is more refined and are of finer scale as compared to other composites. Clustering is also observed at some places. The eutectic silicon colonies network is observed. The majority of eutectic silicon is acquiring globular morphology and eutectic colonies are interconnected.

Overall analysis of structure indicates that microstructure is refined whereas eutectic silicon are having blunted and globular morphological features. This refinement may lead to better tribological and mechanical properties of the composite. The colonization of eutectic silicon in the vicinity of the particles enhances wear resistance of material. The reinforced particles are fairly distributed in the alloy matrix. The good bonding between particles and alloy matrix is also revealed in the microstructural analysis. Moreover, porosity is at minimum level and not observed in the optical examination, although clustering is seen at same places in the composite. Microstructure analysis shows that addition of SiC has a pronounced effect on the microstructure refinement, particularly eutectic silicon. The degree of microstructure and eutectic silicon refinement increases in accordance with the increase of SiC reinforced particle percentage. The most prominent feature observed in all composites is the absence of dendritic growth, which is accounted for two-step stir casting processing of the composites.

3.2. Microhardness

The microhardness measurement at different phases of composite has been carried out to know the effect of reinforced particulates on the alloy matrix. It is observed that the hardness of aluminum composites increases with increase in SiC particle content as given in Table 4.

Microhardness measurements have been carried out on the embedded reinforced particles as well as in the vicinity of particles and matrix. Reinforced particles show high hardness, which decreases as we move away from particle to matrix. The high hardness at particle/matrix interface indicates good interfacial bonding between particle and alloy matrix. Composite-B shows high microhardness value at particle, interface and matrix in comparison to other composites, which is achieved by good interfacial bonding and refinement of microstructure.

3.3. Wear characteristics

Fig. 2(a) represents the variation of the wear rate as a function of temperature for DRP and SRP composites at 1 kg load. It is evident from this figure that at low load (1 kg), wear rate of both DRP and SRP composites decreases with increase in temperature from 50 °C to 200 °C though its variation is nominal. As the temperature

Table 4
Variation of microhardness (Hv).

Composite	Particle	Interface	Matrix
A	735.03	129.42	69.85
B	730.28	138.31	93.06
C	695.08	117.23	70.83
D	677.23	127.21	71.28
E	724.21	129.31	76.03

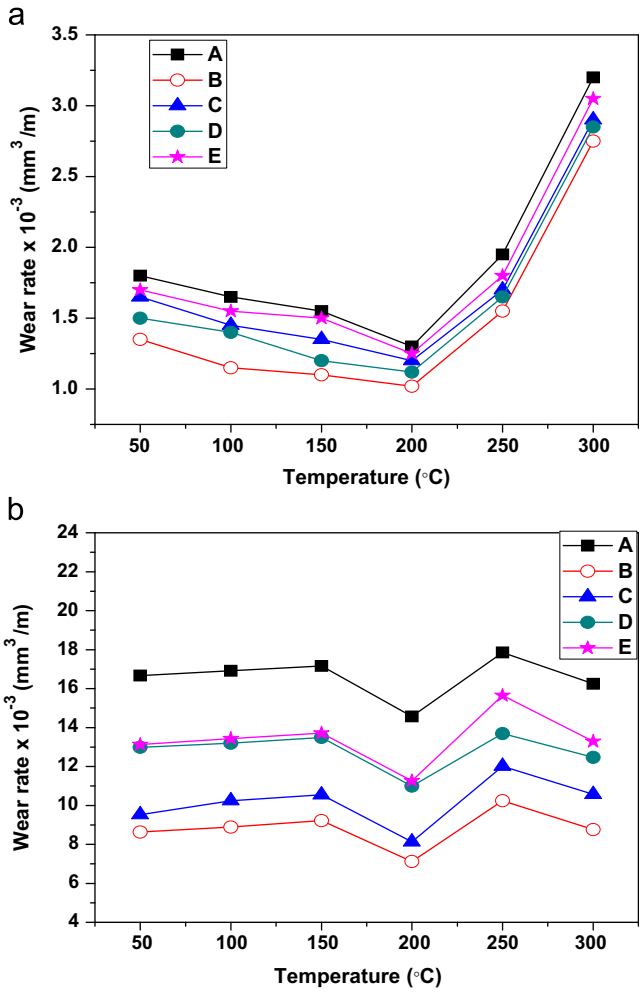

Fig. 2. Wear rate against the temperature of the composites with (a) 1 kg load and (b) 5 kg.

is increased, Al matrix expands and holds the particle more tightly. Under these conditions, reinforced particles offer more resistance to wear causing a decrease in wear rate. Here adhesive wear mechanism dominates up to 200 °C. However, at higher temperature, due to the formation of oxide layers between the sample surface and counter surface of the steel disc wear rate of the composites decreases sharply. The decrease in wear rate at elevated temperature is because of the fact that at low load the asperities on the surface are elastically deformed. It is further noted that DRP composites offer lower wear rate in comparison to that of SRP composites. It is interesting to note that above 200 °C the wear rate of all composites increases gradually as temperature is increased. The composites show transition from mild to serve wear at above 200 °C temperature. Martin et al. [19] have measured the wear rate for 2618 Al alloy reinforced with 15 vol% SiC in the temperature range 20 °C to 200 °C where a transition from mild to severe wear was observed. Zhang and Alpas [20] have suggested that the critical transition (from mild to severe) of wear mode occurs at temperature corresponding to $0.4T_m$ where T_m is melting point of alloy (T_m=650 °C, melting temperature for LM13 alloy). At this critical temperature, thermally activated deformation process becomes active which may lead to softening of the material adjacent to the contact surfaces.

The wear rate of all composites at high load (5 kg) with variation in temperature from 50 °C to 300 °C is shown in Fig. 2(b). It was observed that wear rate increases slightly from 50 °C to 150 °C and then decreases at 200 °C temperatures for both DRP and SRP composites. At the initial stage of sliding, the alloy matrix expands and become soft compared to a later stage. The tightened particles are removed under the influence of high load and got detached exposing fresh matrix surface. However, the alloy gets strain hardened due to continuous sliding under an applied load after a certain sliding distance, which further offers resistance to wear and less loss is observed in between 50 °C and 150 °C at higher load condition. Between 150 °C and 200 °C formation of oxide layer on the surface of pin protects the surface causing a decrease in wear rate [19]. Above 200 °C the transition from mild to severe wear occurs and matrix becomes more soft causing detachment of the formed oxide layer by delamination mechanism [21]. Increment in wear rate is because of the removal of large wear particles by the process of plastic deformation of the surface layer, nucleation of subsurface crack followed by crack propagation due to continuous sliding action. Again, it is interesting to note that with increment in temperature from 250 °C to 300 °C, the wear rate of DRP and SRP composites gradually decreases. At higher load and high temperature, the chip out debris stick at the edges (due to softening effect of matrix at higher temperature) get removed easily from the edges resulting a decrement in wear rate. In all the tests composite-B is continuously exhibiting better wear resistance at all temperature. Better microhardness of the interface can be directly correlated to the good bonding achieved by the reinforcement with the matrix. Composite-D also exhibits better wear resistance as compared to composite-A in which only zircon sand particle is reinforced. However, composite-B also exhibits better wear resistance as compared to composite-E in which only silicon carbide particles are reinforced. Composite-B having a combination of 3.75% silicon carbide and 11.25% zircon sand particles shows better wear resistance as compared to all composites at high load (5 kg) with an increase in temperature from 50 °C to 300 °C. All the composites show the increment in wear rate with increase in temperature from 200 °C to 250 °C followed by further decrease with increasing temperature up to 300 °C at 5 kg load. This variation in wear rate is because of removal of oxide layer due to continuous sliding action, which results in direct metal-to-metal contact. Rajaram et al. [21] pointed out that the formation of oxide films at high temperature reduces the wear rate by avoiding direct metal-to-metal contact. The oxide film may be removed due to continuous sliding actions, which results in direct metal-to-metal contact, and exposing new surface to the environment.

At elevated temperatures, the strain transfer phenomenon to the interfaces becomes less effective as the surrounding matrix alloy begins to soften. At this stage the fracturing of the reinforced particles may mainly occur by crushing and grinding action against each other and also the steel counterface in the soft matrix alloy. As a result, major component of composite may get damaged at elevated temperatures under tensile strain conditions and may lead to formation and growth of void within the matrix alloy [22]. There is a decrement in wear rate at 300 °C for all composites, which is mainly due to the presence of steel debris between the sliding surface. Wilson and Alpas [22] have observed similar behavior around 300 °C for Al matrix composite. They suggested that there is a possible mild to severe wear transition occurring in the counterface steel itself, at or near a temperature of 300 °C. Once severe wear and seizure effects arise in with the steel during sliding contact, the steel debris generated by this process would be transferred to the opposing wear surface of the composite specimen leading to negative or minimum composite wear rate.

After analyzing wear behavior of composites at low loads (1 kg) and high load (5 kg) at different temperature, it is clear that dual reinforcement particle (DRP) mixed in definite proportion is very much effective process for enhancing wear resistance. Silicon carbide particles are better for wear behavior as compared to zircon sand particles as reinforcement in LM13 alloy. Composite-B exhibits better wear behavior due to high microhardness of the interface between particle and matrix. Good interfacial bonding is necessary for better wear behavior as load transfer occurs through interface and also debonding of reinforcement particles results in increase in wear rate.

3.4. Morphological analysis of worn surface and debris

The morphologies of worn out surface of pins and debris offer clues to the wear mechanisms involved in sliding wear of the samples. SEM micrographs of worn surfaces of composites at different operating temperatures are shown in (Figs. 3–6). The worn surfaces of composite-A tested at 200 °C temperature with 1 kg load are shown in Fig. 3(a). The scratches and shallow grooves parallel to the sliding direction on the worn surfaces of the composites are observed in the micrograph. The fracture of oxide layers are clearly observed in SEM micrograph. At 300 °C, worn surface shows plastic deformation. The ploughing marks are more deeper as compared to 200 °C temperatures and

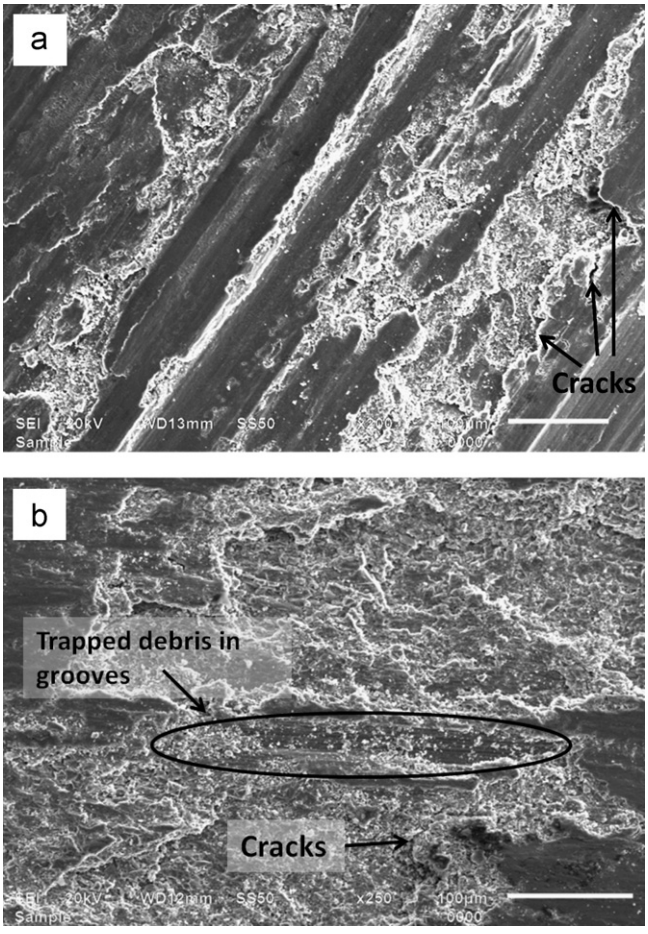

Fig. 3. SEM images of wear track of composite-A at1 kg load with (a) 200 °C and (b) 300 °C.

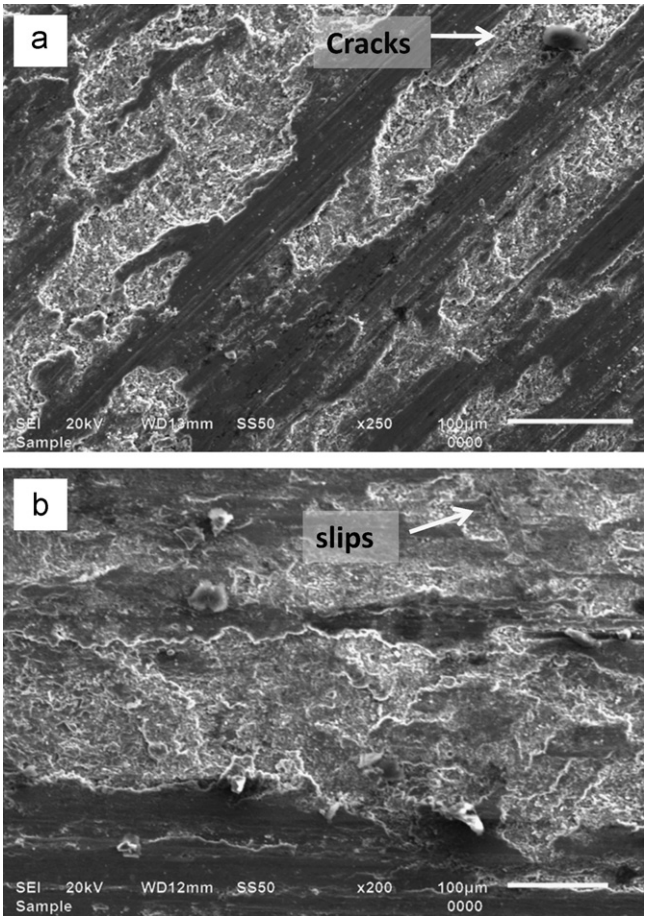

Fig. 4. SEM images of wear track of composite-B at 1 kg load with (a) 200 °C and (b) 300 °C.

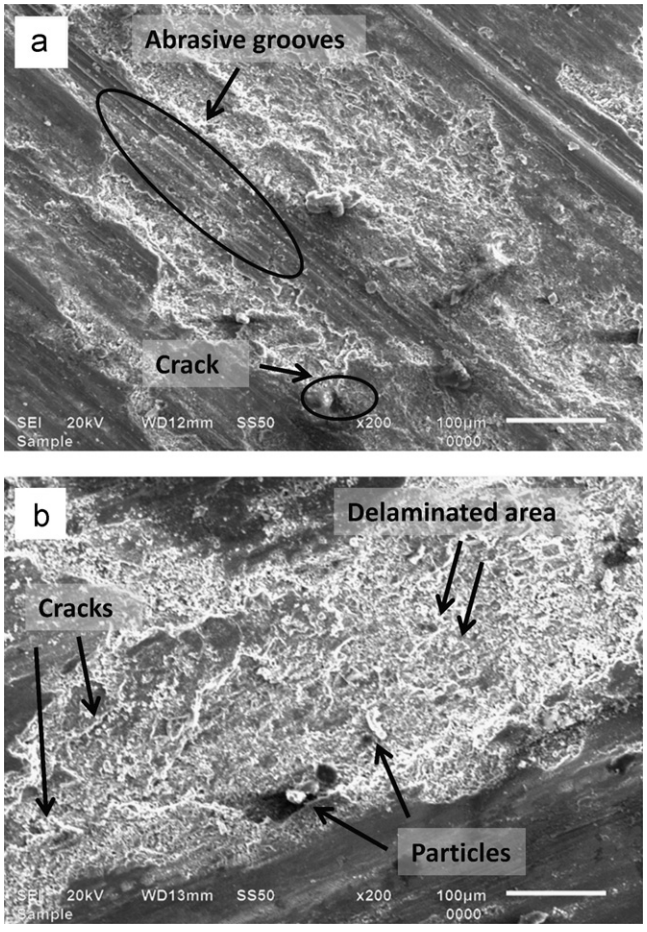

Fig. 5. SEM images of wear track of composite-A at 5 kg load with (a) 200 °C and (b) 250 °C.

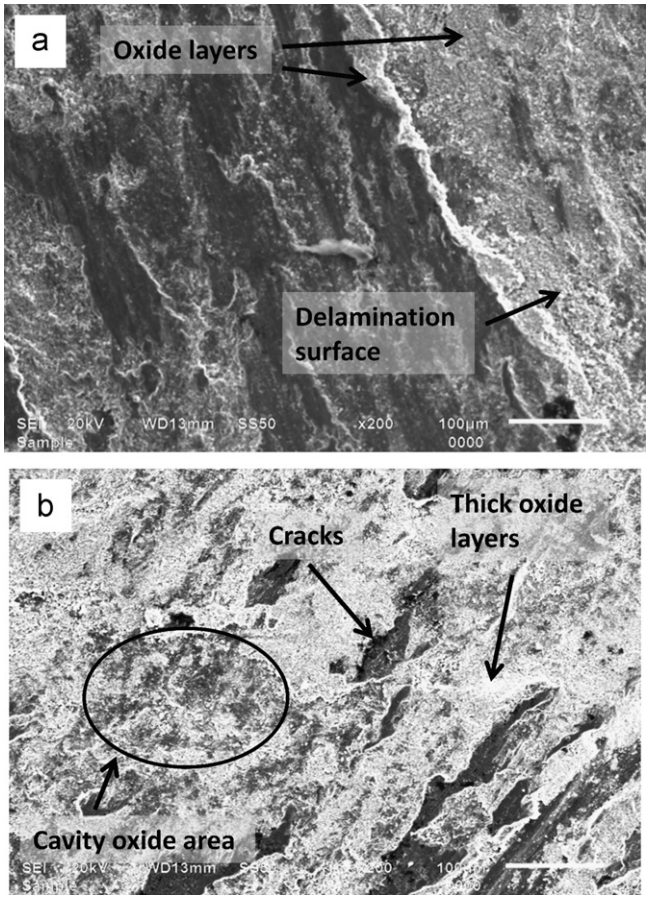

Fig. 6. SEM images of wear track of composite-B at 5 kg load with (a) 200 °C and (b) 250 °C.

generation of cavities due to delamination of surface materials occurs as can be seen in Fig. 3(b). The formations of such grooves during the sliding of composites are observed on numerous occasions, which are linked to the process of delamination. Onset of transition of mild to severe wear is observed at high temperature by formation and delamination of oxide layers on the wear surface (at 200 °C) as shown in Fig. 4(a). The plastic deformation of the surface layer and crack propagation are presents in Fig. 4(a) and (b). This is responsible for increase in wear rate. In composite-B continuous longitudinal grooves parallel to the sliding direction on the worn surfaces of the composites are shown in Fig. 5(a). The wavy pattern of these grooves results from the ploughing action of particles followed by plastic deformation during the wear test. The SEM micrograph of sample (Fig. 5(b)) at operating temperature of 250 °C shows large plastic deformation in addition to abrasion action of zircon particles showing high degree of flow of materials along the sliding direction, which generates cavities due to tearing and delamination of surface materials causing a transition from mild to severe wear at high temperature. At higher load sub-surface delamination is produced by coalescence of these wear cracks as shown in Fig. 6(a). At 250 °C temperature the worn surface shows the oxide cover over a thick area along with fresh surface of aluminum as shown in Fig. 6(b). The depth of microploughing increased with increasing temperature (250 °C) and new large cavity oxide area is created at this temperature.

Mondal et al. [23] suggested that the flow of material in wavy form (serration) and large cavity are due to delamination. At high temperature, the greater degree of softening of surface materials, partial melting of worn surface and localized adhesion between specimen surface and counter body are responsible for the mild to severe wear followed by delamination of the composites as shown in Figs. 5 and 6(a). With increase in temperature up to 250 °C, the subsurface and surface cracks are visible. The crack propagation is along the sliding direction and also in perpendicular direction of sliding, which result in material removal by delamination. Sudarshan and Surappa [24] in their work have reported that the void nucleation around the second phase particles in the deformed region and their subsequent growth and linkage parallel to surfaces lead to the delamination of subsurface layers and finally to the material loss in the form of plate like debris. The depth of microploughing is increased on increasing load to 5 kg where contact asperities change the shape. Consequently, the size and depth of the grooves become greater at this stage. At higher

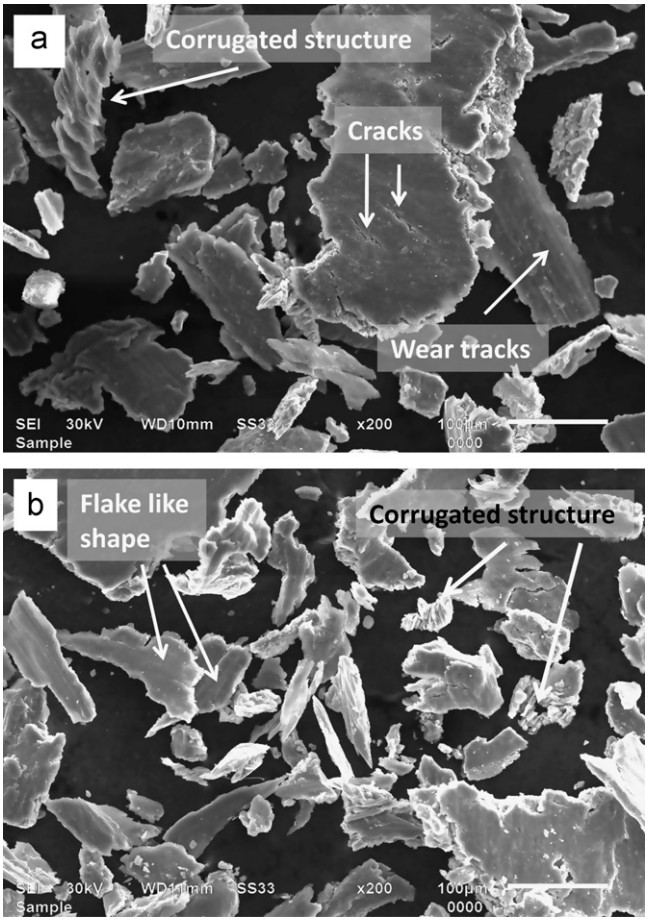

Fig. 7. SEM images of wear debris of composite-A at1 kg load with (a) 200 °C and (b) 300 °C.

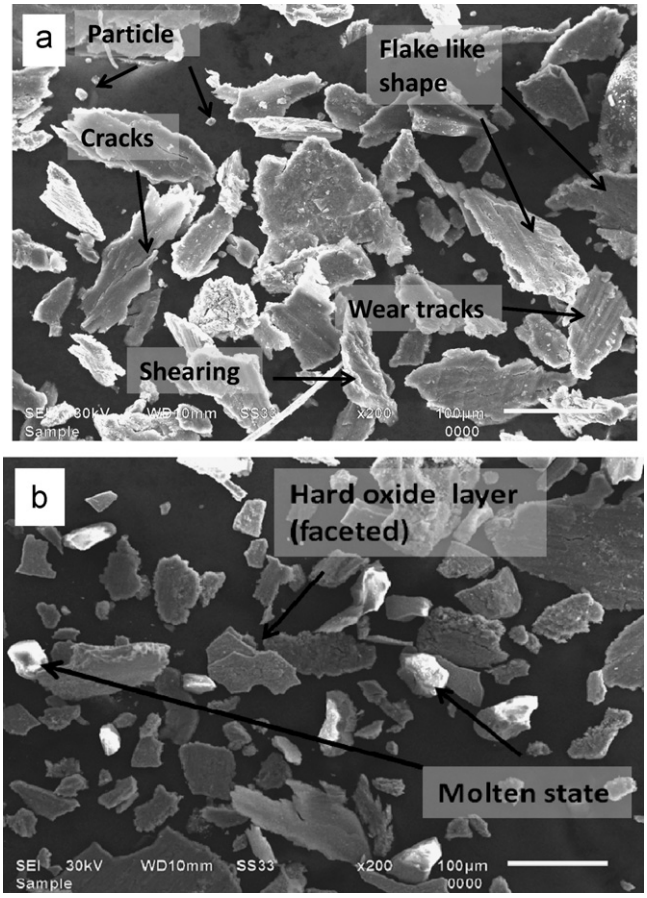

Fig. 8. SEM images of wear debris of composite-B at1 kg load with (a) 200 °C and (b) 300 °C.

load the material removal is caused by micro cutting and delamination, which is resulted from the microcracks.

4. Analysis of debris

SEM analyses of the wear debris were performed to identify the mode of wear mechanism by analysis of the morphology of the debris. Wear debris for composite-A collected at 1 kg load for 200 °C and 300 °C temperature are shown in Fig. 7(a) and (b), respectively. The size and shape of collected debris change with increase in temperature from 200 °C to 300 °C at 1 kg load. At 200 °C temperature flakes like shape debris have larger size compared to 300 °C. At this temperature, corrugated structure was observed in some debris shown in Fig. 7(a), which may occur due to constant rubbing between wear surfaces of sample and counterface. The larger size and cracked debris with corrugated structure was observed in Fig. 7(b). At 300 °C temperature, these debris are responsible for higher wear rate. The elongated delaminated flakes in debris show groove marks indicates that they have come out due to shearing of layer in Fig. 8(a), which occurred in direction of force applied. At 300 °C temperature, plate-like shape debris has smaller size compared to 200 °C temperature at 1 kg load in Fig. 8(b). The molten state of debris and small size of debris are present in Fig. 8(b) at 300 °C temperature. The hard oxide layer (faceted) is present in Fig. 8(b). It indicates that severe wear dominates for alloy at this high temperature condition. Presence of partially molten state of debris supports to increase in the wear rate of the composite at high temperature. Spherical shaped wear debris can be caused by several sources including entrapment of wear debris in surface depression, inclusions from base metal, local melting and air born contamination [25]. Material containing particles is also visible with debonded reinforced particles in Fig. 9(a). Flakes generated by cutting action along with delaminated flakes are also observed. Layered structure of debris in Fig. 9(a) is due to the removal of material in continuous sliding action during the wear test. The flakes having microcracks, which show that, the removal of material is also due to crack propagation and delamination. As temperature is increased up to 250 °C, severe wear at high load and high temperature is observed in Fig. 9(b) for composite-B. Presence of micro cutting and metal fiber in Fig. 9(b), supports to higher wear rate. The smaller debris are agglomerated along the larger debris due to thermal mechanical welding by repetitive forces during sliding [26]. At high load and high temperature, the thread type debris created during the pulling out of aluminum metal is observed in Fig. 9(b). The oxides debris are created at high temperature with high load. At a much higher temperature (250 °C) these oxides (Al_2O_3/Fe_2O_3) debris

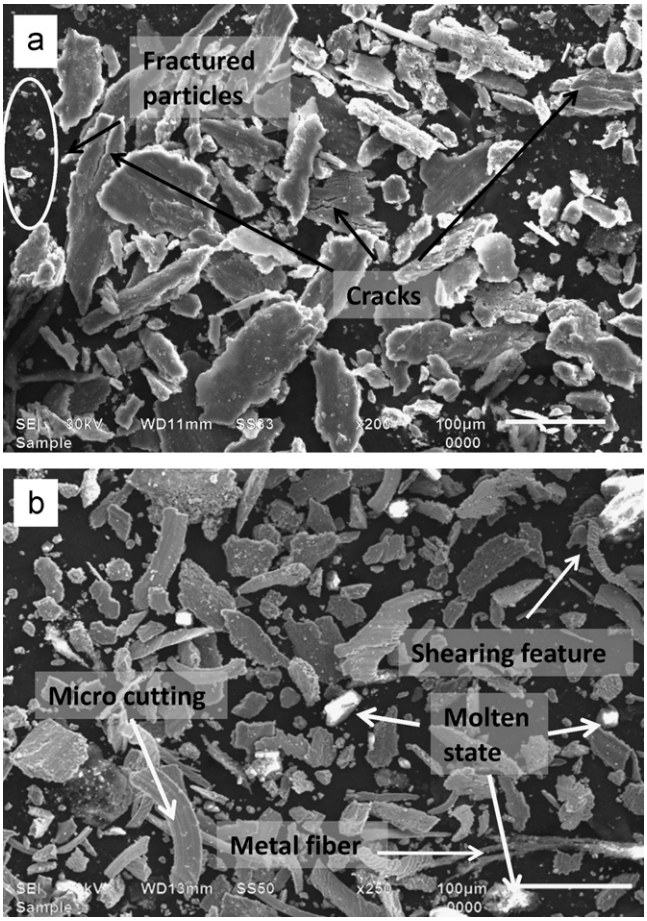

Fig. 9. SEM images of wear debris of composite-A at 5 kg load with (a) 200 °C and (b) 250 °C.

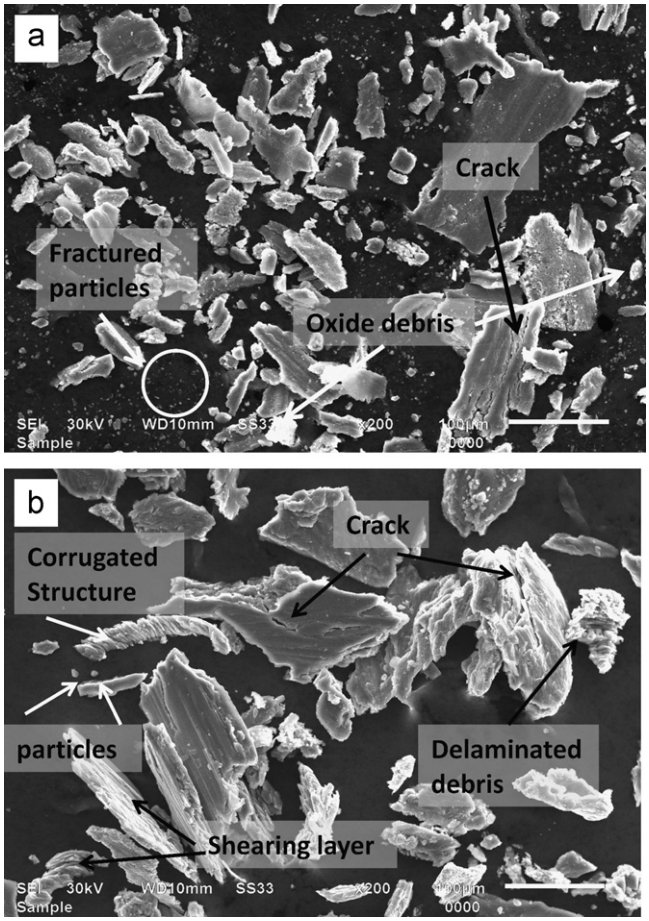

Fig. 10. SEM images of wear debris of composite-B at 5 kg load with (a) 200 °C and (b) 250 °C.

help to reduce the wear rate of composite at high load as they keep on rotating inside the grooves. In this figure, the small size debris with fine thickness and some corrugated structure are observed. The step clearly observed on delaminated debris in Fig. 9(a) and (b) may be due to slip to the Al and SiC particles interfaces due to constant rubbing between the wear surfaces [27]. Fig. 10(a) shows the SEM image of debris of composite-B tested at 200 °C with 5 kg load. Delaminated debris with cracks and fractured reinforced particle as along with oxide debris are observed in Fig. 10(b). Oxide debris help to reduce the wear rate of composite-B at high load. Due to softening of the matrix in composite-B, particle is inserted in the matrix, which supports to the delamination of some large debris. Fig. 10(b) shows the cracked large size debris (corrugated structure) collected for composite-B tested at 5 kg load with 200 °C temperature. However, some plate like debris with large size are also observed in this micrograph, which indicate the presence of both abrasive and adhesive wear mechanism. The elongated delaminated debris having grooves indicate that it comes out due to shearing action of the layer in the direction of applied force. In Fig. 10(b), shape and sizes of debris (crashed type debris) indicate that the matrix becomes soft and onset of transition from mild to severe wear occurs at the high temperature. It is also observed that these debris undergo multiple ploughing action causing cracking in it. Moreover, it appears that some of the debris have undergone melting. This is because of generation of high temperature during sliding action in wear test. The sub-surface cracks may be responsible for generating the wear debris. These wear scars are the primarily characteristic of abrasive wear. The size of craters and wear debris do not match. In general, wear debris particles are very small than the craters [26]. Under low load and dry wear sliding conditions, wear debris is generally spherical and friable in nature while at high load the wear debris is found to be metallic. Presence of large amount of flake type debris suggests that delamination is the predominating mechanism at high pressure and there is no correlation between size of particles and silicon content. SEM micrographs showing the mechanically mixed layer formed on the contact surface of the composites shows a bimodal size distribution of fine spherical particles and larger plate-like debris.

5. Conclusion

The effect of high temperature on wear behavior of LM13 alloy with DRP and SRP reinforcement was studied and the results are summarized as follows:

1. Dual reinforcement particles have different functions in the composite. Silicon carbide refines the eutectic silicon

whereas zircon sand provides good interfacial bonding. Zircon sand and silicon carbide particles also provide effective nucleation site for eutectic silicon. The eutectic silicon is having globular morphology in the vicinity of particles.

2. The combination of zircon sand and silicon carbide particle in a ratio of (1:3) reinforcement in the composite exhibits better wear resistance as compared to other combinations at all the temperature at low and high load both.
3. Study reveals that the dual reinforcement particle enhances the wear resistance as compared to single reinforcement particle if mixed in a definite proportion.
4. Wear behavior of the composites is increased linearly with increasing the operating temperature at high load. This effect is due to formation of the oxide film and glazing layer on sliding components. These layers prevent the direct metal-to-metal contact of sliding surfaces during sliding.

Acknowledgement

The authors are thankful to Armament Research Board (ARMREB), Defence Research and Development Organization (DRDO), India for providing financial support under the letter no. ARMREB/MAA/2008/105 for this study.

References

[1] S. Bajwa, W.M. Rainforth, W.E. Lee, Sliding wear behaviour of SiC/Al_2O_3 nano composites, Wear 259 (2005) 553–561.
[2] S. Das, K. Das, S. Das, Abrasive wear behavior of Al–4.5 wt% Cu/(zircon sand + silicon carbide) hybrid composite, Journal of Composite Materials 43 (2009) 2665–2672.
[3] K. Kaur, O.P. Pandey, Dry sliding wear behavior of zircon sand reinforced Al–Si alloy, Tribology Letters 38 (2010) 377–387.
[4] Y.Q. Wang, A.M. Afsar, J.H. Jang, K.S. Han, J.I. Song, Room temperature dry and lubricant wear behaviors of $Al_2O_{3f}/SiC_p/Al$ hybrid metal matrix composites, Wear 268 (2010) 863–870.
[5] S. Suresha, B.K. Sridhara, Effect of addition of graphite particulates on the wear behavior in aluminum–silicon carbide-graphite composites, Materials in Design 31 (2010) 1804–1812.
[6] H. Ahlatci, T. Kocer, E. Candan, H. Cimenoglu, Wear behaviour of $Al/(Al_2O_{3p} + SiC_p)$ hybrid composites, Tribology International 39 (2006) 213–220.
[7] S. Das, K. Das, S. Das, Abrasive wear of zircon sand and alumina reinforced Al–4.5 wt% Cu alloy matrix composites-A comparative study, Composites Science and Technology 67 (2007) 746–751.
[8] K.R. Ahmad, S.B. Jamaludin, L.B. Hussain, Z.A. Ahmad, The influence of alumina particle size on sintered density and hardness of discontinuous reinforced aluminum metal matrix composite, Jurnal Teknologi 42 (A) (2005) 49–57.
[9] N. Ozdemir, F. Yakuphanoglu, The effects of particle size and volume fraction of Al_2O_3 on electronic thermal conductivity of α-Al_2O_3 particulate reinforced aluminum composites (Al/Al_2O_3-MMC), International Journal of Advanced Manufacturing Technology 29 (2006) 226–229.
[10] Y. Wang, H.Y. Wang, K. Xiu, Hong-Ying Wang, Q.C. Jiang, Fabrication of TiB_2 particulate reinforced magnesium matrix composites by two-step processing method, Materials Letters 60 (2006) 1533–1537.
[11] W. Zhou, Z.M. Xu, Casting of SiC reinforced metal matrix composites, Journal of Materials Processing Technology 63 (1997) 358–363.
[12] V. Sharma, S. Kumar, R.S. Panwar, O.P. Pandey, Microstructural and wear behavior of dual reinforced particle (DRP) aluminum alloy composite, Journal of Materials Science 47 (2012) 6633–6646.
[13] S. Kumar, V. Sharma, R.S. Panwar, O.P. Pandey, Wear behavior of dual particle size (DPS) zircon sand reinforced aluminum alloy, Tribology Letters 47 (2012) 231–251.
[14] J. Hashim, The production of cast metal matrix composite by a modified stir casting method, Jurnal Teknologi 35A (2001) 9–20.
[15] S.K. Chaudhury, A.K. Singh, C.S. Sivaramakrishnan, S.C. Panigrahi, Wear and friction behavior of spray formed and stir cast $Al_2Mg_{11}TiO_2$ composites, Wear 258 (2005) 759–767.
[16] E.G. Okafor, V.S. Aigbodion, Effect of zircon silicate reinforcements on the microstructure and properties of as cast Al–4.5Cu matrix particulate composites synthesized via squeeze cast route, Tribology in Industry 32 (2010) 31–37.
[17] R.S. Panwar, O.P. Pandey, Analysis of wear tracks and debris of stir cast LM13/Zr composite at elevated temperatures, Materials Characterization 75 (2013) 200–213.
[18] J. Hashim, L. Looney, M.S.J. Hashmi, Particle distribution in cast metal matrix composites—Part 1, Journal of Materials Processing Technology 123 (2002) 251–257.
[19] M.A. Martinez, A. Martin, J. Llorca, Wear of SiC-reinforced Al-matrix composites in the temperature range 20–200 °C, Wear 193 (1996) 169–179.
[20] J. Zhang, A.T. Alpas, Wear Regimes and transition in Al_2O_3 particulate-reinforced alloys, Materials Science and Engineering A 161 (1993) 273–284.
[21] G. Rajaram, S. Kumaran, T. Srinivasa Rao, High temperature tensile and wear behaviour of aluminum silicon alloy, Materials Science and Engineering A 528 (2010) 247–253.
[22] S. Wilson, A.T. Alpas, Effect of temperature on the sliding wear performance of Al alloys and Al matrix composites, Wear 196 (1996) 270–278.
[23] D.P. Mondal, S. Das, R.N. Rao, M. Singh, Effect of SiC addition and running-in wear on the sliding wear behaviour of Al–Zn–Mg aluminium alloy, Materials Science and Engineering A 402 (2005) 307–319.
[24] M.K. Surappa Sudarshan, Dry sliding wear of fly ash particle reinforced A356 Al composites, Wear 265 (2008) 349–360.
[25] A.W.J. De Gee, A note on the relation between friction and wear, Wear 65 (1981) 397–398.
[26] A.J. Clegg, A.A. Das, Wear of a hypereutectic aluminium–silicon alloy, Wear 43 (1977) 367–373.
[27] S. Kumar, R.S. Panwar, O.P. Pandey, Wear behavior at high temperature of Dual particle size (DPS) zircon sand reinforced aluminum alloy composite, Metallurgical and Materials Transactions A: Physical Metallurgy and Materials Science (2012) http://dx.doi.org/10.1007/s11661-012-1504-y.